Thin Solid Films 552 (2014) 86–91

Contents lists available at ScienceDirect

Thin Solid Films

journal homepage: www.elsevier.com/locate/tsf

Formation of ferromagnetic germanides by solid-state reactions in 20Ge/80Mn films

V.G. Myagkov [a,b,*], V.S. Zhigalov [a,b], A.A. Matsynin [a], L.E. Bykova [a], Yu.L. Mikhlin [c], G.N. Bondarenko [c], G.S. Patrin [a,d], G.Yu. Yurkin [a,d]

[a] Kirensky Institute of Physics, Russian Academy of Sciences, Siberian Branch, Krasnoyarsk 660036, Russia
[b] Reshetnev Siberian State Aerospace University, Krasnoyarsk 660014, Russia
[c] Institute of Chemistry and Chemical Technology, Russian Academy of Sciences, Siberian Branch, Krasnoyarsk 660049, Russia
[d] Siberian Federal University, Krasnoyarsk 660041, Russia

ARTICLE INFO

Article history:
Received 9 January 2013
Received in revised form 5 November 2013
Accepted 15 December 2013
Available online 22 December 2013

Keywords:
Manganite–germanium
Solid state reaction
First phase
Mn5Ge3 alloy
Carbon impurity
Oxygen impurity
Annealing
Magnetic anisotropy

ABSTRACT

Solid state reactions between Ge and Mn films are systematically examined using X-ray diffraction, photoelectron spectroscopy, and magnetic and electrical measurements. The films have a nominal atomic ratio Ge:Mn = 20:80 and are investigated at temperatures from 50 to 500 °C. It is established that after annealing at ~120 °C, the ferromagnetic Mn_5Ge_3 phase is the first phase to form at the 20Ge/80Mn interface. As the annealing temperature increases to 300 °C, the weak magnetic Mn_5Ge_2 + Mn_3Ge phases simultaneously begin to grow and they become dominant at 400 °C. Increasing the annealing temperature to 500 °C leads to the formation of the ferromagnetic phase with a Curie temperature T_C ~ 350–360 K and magnetization 14–25 kA/m at room temperature. The X-ray diffraction study of the samples shows the reflections from the Mn_5Ge_3 phase, and the photoelectron spectra contain the oxygen and carbon peaks. The homogeneous distribution of oxygen and carbon over the sample thickness suggests that the increased Curie temperature and magnetization are related to the migration of C and O atoms into the Mn_5Ge_3 lattice and the formation of the Nowotny phase $Mn_5Ge_3C_xO_y$. The initiation temperature (~120 °C) is the same in the Mn_5Ge_3 phase with the solid-state reactions in the Ge/Mn films as well as in the phase separation in the Ge_xMn_{1-x} diluted semiconductors. Thus, we conclude that the synthesis of the Mn_5Ge_3 phase is the moving force for the spinodal decomposition of the Ge_xMn_{1-x} diluted semiconductors.

1. Introduction

An important goal in spintronics is to create media with high-efficiency spin injection into nonmagnetic semiconductors. Ferromagnetic materials are the main candidates for spin injection sources. Their drawback, however, is that nonmagnetic layers form during deposition onto Si and Ge substrates. In recent years there has been keen interest in the synthesis of Mn_5Ge_3 thin films as spin injection sources [1–3]. The ferromagnetic Mn_5Ge_3 phase has a Curie temperature above room temperature (T_C = 304 K) as well as sufficiently high spin polarization (P = 42 ± 5%) [4]. This phase is grown on Ge(111) substrates by solid phase epitaxy (SPE), with the deposition of Mn at room temperature followed by annealing [2,3,5–11]. Thus, in the epitaxial Mn_5Ge_3/Ge(111) samples, the ferromagnetic Mn_5Ge_3 compound can potentially be applied as a source of spin injection into the Ge layer.

The properties of the materials that are important in practical applications are high magnetization, high Curie temperature, and thermal stability. A promising approach to enhancing the Curie temperature is to form the $Mn_5Ge_3C_x$ compound by doping the Mn_5Ge_3 with carbon [5–7,12–17]. As shown in Gajdzik et al. [17], T_C grows with the doping level and attains its maximum value T_C = 442 K at x ≥ 0.5. The SPE growth technique is a special case of the initiation of the solid-state reaction between Mn and Ge at the Ge/Mn interface [18–20]. It is noteworthy that the ferromagnetic Mn_5Ge_3 phase forms not only from the solid-state reactions in the Ge/Mn samples, but also during the low-temperature (~120 °C) spinodal decomposition in Mn_xGe_{1-x} (x < 0.05) diluted semiconductors [21–26]. Recently, we have shown the sequential formation of the Mn_5Ge_3 and $Mn_{11}Ge_8$ phases in polycrystalline 80Ge/20Mn nanofilms having 80Ge:20Mn atomic composition at initiation temperatures of ~120 and 300 °C, respectively [18].

Investigations continue to examine the scenarios and mechanisms underlying the chemical interaction of Mn and Ge and the formation of the ferromagnetic Mn_xGe_{1-x} phases at low temperatures. Information is lacking regarding the effect of gasses on the synthesis of the Mn_5Ge_3 compounds and their magnetic characteristics. To analyze the

* Corresponding author at. Kirensky Institute of Physics, Russian Academy of Sciences, Siberian Branch, Krasnoyarsk, 660036 Russia. Tel.: +7 391 2494681.
E-mail address: miagkov@iph.krasn.ru (V.G. Myagkov).

0040-6090/$ – see front matter © 2013 Elsevier B.V. All rights reserved.
http://dx.doi.org/10.1016/j.tsf.2013.12.029

formation of the magnetic phases in the Mn–Ge system, it is necessary to thoroughly investigate the regularities of the solid-state reactions between elemental Mn and Ge.

In this study, we investigate phase formation in 20Ge/80Mn film samples after annealing at temperatures up to 500 °C in a vacuum at a residual pressure of 10^{-4} Pa. We demonstrate the formation of the 20Ge/80Mn → (~120 °C) Mn_5Ge_3 → (~300 °C) (Mn_5Ge_2 + Mn_3Ge) → (~500 °C) $Mn_5Ge_3C_xO_y$ phase sequence. Then, we present the magnetic characteristics of the $Mn_5Ge_3C_xO_y$ phase and discuss general mechanisms in the formation of the Mn_5Ge_3 phase during solid-state synthesis in Ge/Mn films and phase separation in $Ge_x Mn_{1-x}$ diluted semiconductors.

1.1. Experimental details

Initial 20Ge/80Mn bilayers are obtained by the sequential thermal deposition of Mn and Ge layers onto glass substrates in a vacuum at a residual pressure of 10^{-6} Pa. The substrates are degassed at 350 °C with the subsequent deposition of Mn layers at 200 °C. The top Ge layers are deposited at room temperature to prevent a reaction between Ge and Mn during deposition. In these experiments, we use samples with a 20Ge:80Mn (hereafter, 20Ge/80Mn) atomic composition and a total thickness of 0.5 μm. The initial 20Ge/80Mn samples are annealed in a vacuum at a residual pressure of 10^{-4} Pa at temperatures from 50 to 500 °C, with a pitch of 50 °C and 30 min exposure at each temperature. The in-plane M–H hysteresis loops were used to measure the magnetization. The saturation magnetization M_S is measured on an MPMS-XL SQUID magnetometer (Quantum Design) in magnetic fields up to 5 T. The formation phases are identified using a DRON-4-07 diffractometer (CuK_α radiation). X-ray photoelectron spectra (XPS) are obtained on a SPECS photoelectron spectrometer (Germany) with the use of an X-ray tube for exciting Mg Kα radiation spectra (1253.6 eV). The relative concentrations of the elements are determined by plain X-ray spectra recorded at the transmission energy of 20 eV on a PHOIBOS 150 MCD9 hemispherical energy analyzer using empirical sensitivity coefficients. Narrow scans are detected at the analyzer transmission energy of 8 eV. The spectra are decomposed using the Gaussian–Lorentzian line shape after nonlinear Shirley background subtraction. Surface etching by argon ions is performed with a SPECS PU-IQE 12/38 scanning gun at an accelerating voltage of 5 kV and an ion current of 15 μA; this corresponds to a surface layer scattering rate of 1–1.5 nm/min. The thicknesses of the Ge and Mn layers are determined by X-ray fluorescence analysis. The resistance is measured by a standard four-probe method. All measurements are performed at room temperature.

2. Results and discussion

The diffraction patterns of the initial 20Ge/80Mn films contain α-Mn reflections (Fig. 1a). The absence of Ge reflections suggests that the top Ge layer grew with fine grains. After annealing at 150 °C, the Mn reflections vanish and the ferromagnetic Mn_5Ge_3 phase reflections arise. This phase becomes dominant after annealing at 250 °C (Fig. 1b). As the annealing temperature increases above 250 °C, the Mn_5Ge_3 phase reflections vanish and new peaks arise that have angular positions and intensities strongly dependent on the heating rate, annealing time, and even minor variations in the composition. Most of the peaks correspond to the weak ferromagnetic κ-Mn_5Ge_2 [ICDD PDF35-1409] and ε-Mn_3Ge [ICDD PDF65-6715] phases that become dominant after annealing at 400 °C. A typical X-ray diffraction pattern is shown in Fig. 1c. At annealing temperatures above 400 °C, some of the X-ray patterns contain the peaks from the ε_1-Mn_3Ge [ICDD PDF65-6514] phase that formed due to the $\varepsilon \rightarrow \varepsilon_1$ transition [27]. The unindexed diffraction peaks possibly correspond to the metastable Mn_xGe_{1-x} phases with a high Mn content, or to the nonequilibrium Mn_3Ge structures [28–30]. The peaks of the non-reacted κ-Mn_5Ge_2,

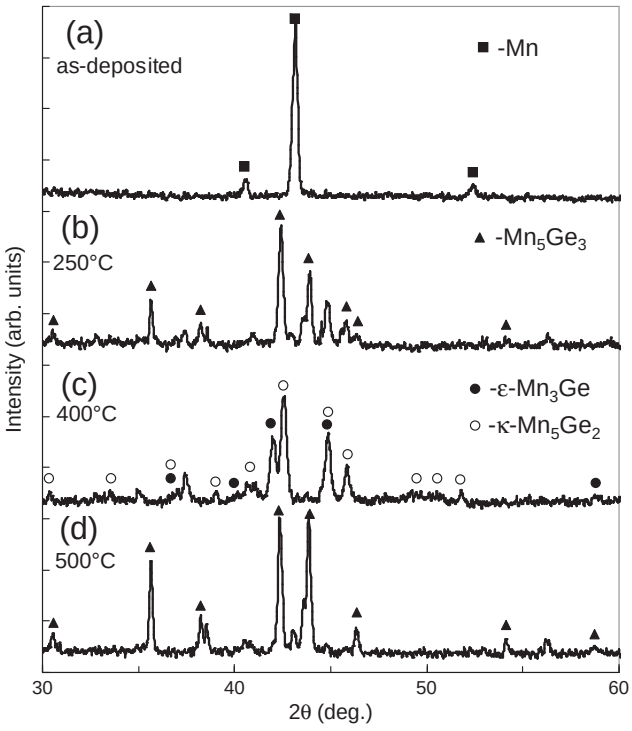

Fig. 1. X-ray diffraction patterns of the 20Ge/80Mn film system: (a) initial sample, (b) sample annealed at 250 °C, (c) 350 °C, and (d) 500 °C.

ε-Mn_3Ge, and ε_1-Mn_3Ge phases remain after annealing at 500 °C; furthermore, weak MnO reflections arise, and the Mn_5Ge_3 phase peaks arise again. The X-ray diffraction patterns of some of the samples contain only the Mn_5Ge_3 reflections (Fig. 1d).

The annealing temperature dependence of the magnetization of the 20Ge/80Mn films (Fig. 2a) shows that there are three temperatures

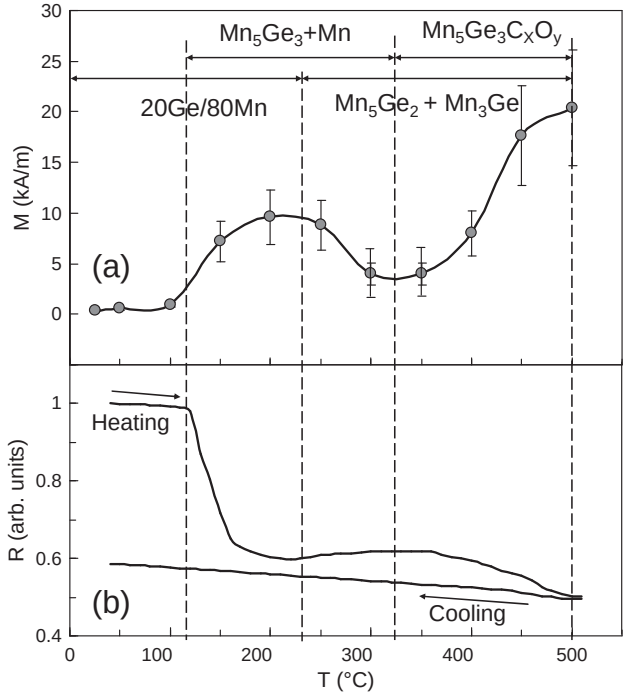

Fig. 2. Annealing temperature dependences of (a) saturation magnetization M_S and (b) resistance R of the 20Ge/80Mn bilayer. The top of the figure shows the temperature boundaries of the existence of the 20Ge/80Mn film system and the Mn_5Ge_3 and $Mn_5Ge_3C_xO_y$ phases.

(250 °C, 350 °C, and 500 °C) at which magnetization reaches an extreme. The experimental magnetization values are scattered; this is likely due to the fact that, apart from the stable phases forming in the Mn-rich side of the Mn–Ge system, the metastable Mn_xGe_{1-x} phases, their structural modifications, and their composition inhomogeneity are induced by annealing.

The initial 20Ge/80Mn samples remain nonmagnetic up to an annealing temperature of 120 °C. The magnetic measurement data show that, after annealing at 120 °C, the samples are characterized by insignificant magnetization. This magnetization strongly grows after annealing at 250 °C. This trend is indicative of the intermixing of the Ge and Mn layers and the solid-state synthesis of a ferromagnetic phase with an initiation temperature T_0^1 ~ 120 °C. When annealing at temperatures above 300 °C, the decrease in the saturation magnetization M_S is related to the formation of weak magnetic compounds with an initiation temperature T_0^2 ~ 300 °C. Surprisingly, upon annealing at temperatures above T_0^3 ~ 400 °C, the saturation magnetization M_S strongly increases, and at 500 °C, reaches its maximum value 14–25 kA/m Fig. 2(a). The evolution of the saturation magnetization with varying annealing temperatures is consistent with the formation of the ferromagnetic Mn_5Ge_3 phase with an initiation temperature T_0^1 ~ 120 °C, and the weak magnetic κ-Mn_5Ge_2 and ε-Mn_3Ge phases above T_0^2 ~ 300 °C.

Fig. 2b shows the annealing temperature dependence of the samples' resistance.

As the temperature increases, the resistance 20Ge/80Mn films change insignificantly and decrease rapidly above ~120 °C. This indicates that there are no significant changes at the Ge/Mn interface up to ~120 °C. The intense intermixing of the Ge and Mn layers and the formation of Mn_5Ge_3 are observed above 120 °C. This is in agreement with the X-ray diffraction patterns, which do not change up to 120 °C, and with XPS studies, in which the migration of Mn atoms into the upper Ge layer is observed at annealing temperatures only above 120 °C. As the annealing temperature further increases, the resistance has its minimum at 150–200 °C and weakly varies in the range 270–370 °C. This is due to the synthesis of the Mn_5Ge_2 and Mn_3Ge phases, which completes at 400 °C. The resistance drop above 370 °C corresponds to the repeated formation of the Mn_5Ge_3 phase. Upon cooling from 500 °C, resistivity smoothly increases with decreasing temperature; this is a typical feature of semiconductor conduction.

The temperature dependences of the saturation magnetization (Fig. 3) confirm the sequential formation of the ferromagnetic Mn_5Ge_3 and weak magnetic Mn_5Ge_2 and Mn_3Ge phases in the 20Ge/80Mn films after annealing at 250 and 400 °C, respectively. The shape of the dependence $M_S(T)$ after annealing at 250 °C (Fig. 3a) indicates the presence of the only magnetic phase with a Curie temperature T_C ~ 300 K; this is typical of the Mn_5Ge_3 phase [3]. The insignificant magnetization of the samples after annealing at 400 °C (Fig. 3b) is due to the remainder of the Mn_5Ge_3 phase and the low magnetizations of the ε-Mn_3Ge, ε_1-Mn_3Ge [27,31], and κ-Mn_5Ge_2 [31] phases. After annealing at 500 °C, the samples with high magnetization have a Curie temperature T_C ~ 350–360 K (Fig. 3c).

The high Curie temperature (Fig. 3b) and the diffraction reflections of the Mn_5Ge_3 phase (Fig. 1c) indicate the effect of the residual gasses on the magnetic properties of the 20Ge/80Mn samples after annealing at 500 °C. It is known that, in C-doped Mn_5Ge_3 films, the saturation magnetization at room temperature and the Curie temperature grow with carbon concentration. At carbon concentrations x ~ 0.6 − 0.7 in $Mn_5Ge_3C_x$ films, the Curie temperature of the latter reaches T_C ~ 360–450 K [12–17]. The doping of amorphous $Ge_{1-x}Mn_x$ films with nitrogen and oxygen impurities improves their magnetic and electrical properties [32]. Ab initio calculations predict the effect of oxygen atoms on the electrical and magnetic properties of Mn-doped Ge [33]. Hydrogenation of the amorphous $Ge_{1-x}Mn_x$ films significantly enhances their saturation magnetization and coercivity [34].

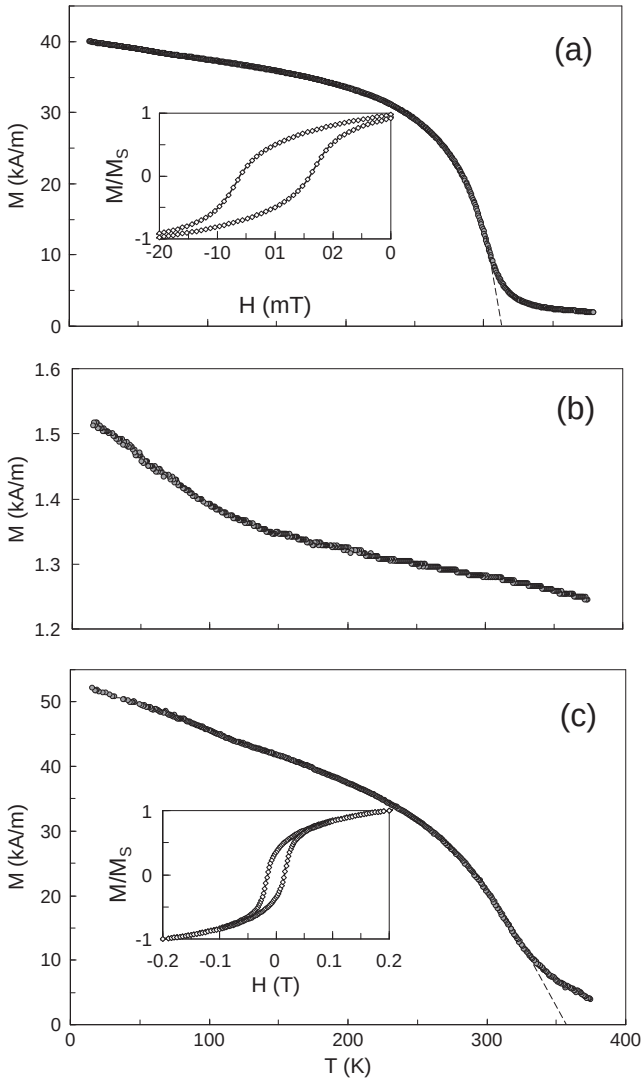

Fig. 3. Temperature dependences of saturation magnetization M_S measured in a magnetic field of 0.5 T for the 20Ge/80Mn film system after annealing at (a) 250 °C, (b) 350 °C, and (c) 500 °C. Insets show in-plane M–H hysteresis loops for Mn_5Ge_3 and $Mn_5Ge_3C_xO_y$ phases.

We investigate the composition and chemical state of Mn, Ge, O, and C over the film depth by applying XPS coupled with Ar + sputtering. XPS study of initial 20Ge/80Mn bilayers reveals the presence of Ge and the absence of Mn after an etching to a depth of 20–30 nm (the spectra are not shown). Fig. 4 presents the relative concentrations of the elements as functions of sputtering time and core-level spectra of the 20Ge/80Mn samples after annealing at 500 °C. After eliminating the oxidized and contaminated surface layer, the distribution of Mn, Ge, O, and C is almost homogeneous, at least to a depth of 50–60 nm (Fig. 4a). At the same time, with the sample annealed at 400 °C, the carbon and oxygen are localized only on the surface (the spectra are not shown). The elemental spectra also change insignificantly with depth. The main contributor to the Mn 2p spectra is the broadband of the multiplet structure typical of MnO (Fig. 4b) [35–38]. This is confirmed by the atomic ratio Mn/O, which is close to unity, and by the oxygen spectrum with a main line near 530.7 ± 0.1 eV. The line O 1s at about 532 eV corresponds to the atoms bound with the oxidized Ge atoms (Fig. 4c) [39]. In the manganese spectrum, there is also a component (or components) with a binding energy of 639–640 eV and a relative intensity of 30%; this can be attributed to germanides and manganese carbide (Fig. 4b). In the Ge 3d spectrum (the Ge 3d core level), the line with a binding energy of 29.4 eV corresponds to

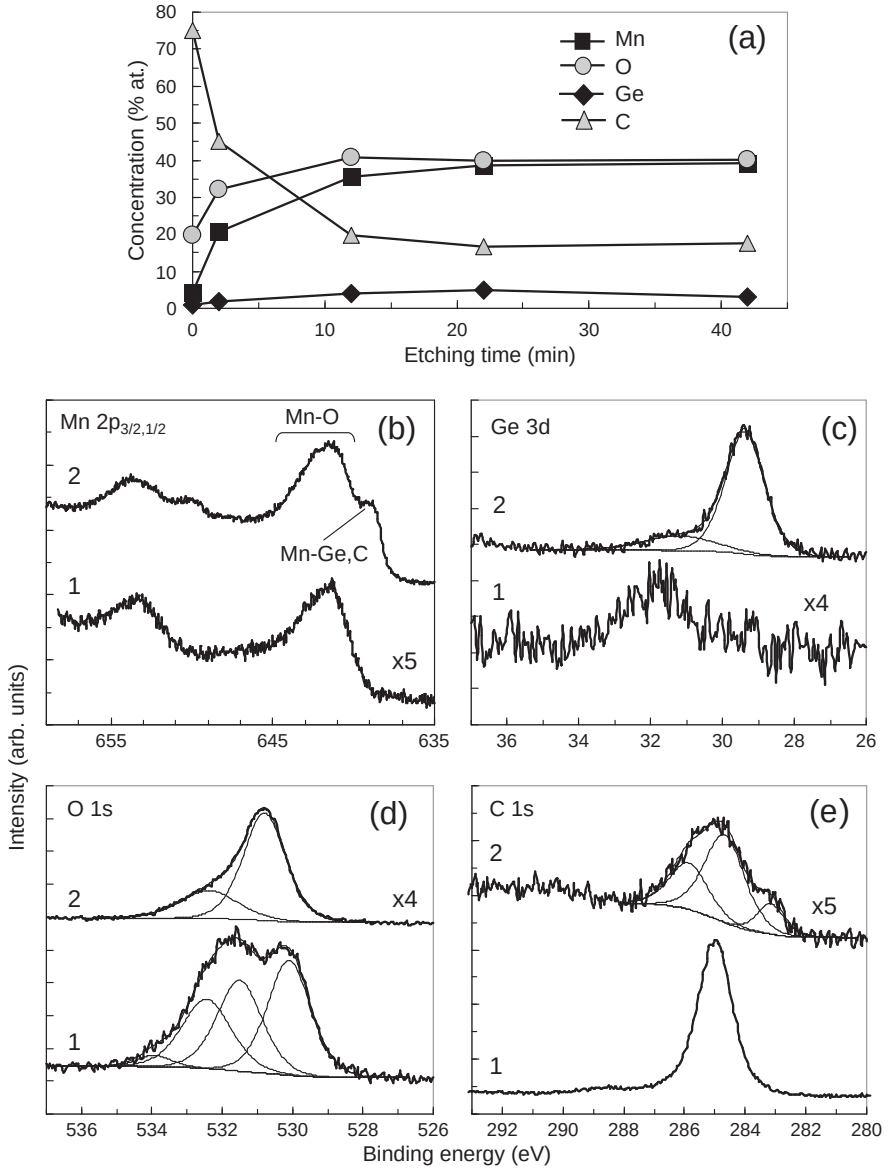

Fig. 4. XPS depth profiles and Mn 2p, Ge 3d, O 1s, and C 1s spectra for the 20Ge/80Mn sample after annealing at 500 °C, (1) before and (2) after Ar^+ sputtering for 12 min.

manganese germanide. The spectrum contains the contribution with a binding energy of ~31.1 eV related to carbon diffused into the Mn_5Ge_3 compound (Fig. 4d) [17]. The Mn/Ge ratio of the corresponding lines with binding energies of 640 and 29 eV is approximately 2.5, which is somewhat higher than that of the Mn_5Ge_3 compound (1.67). This is apparently explained by the presence of the unreacted phases of the Mn_5Ge_2 and Mn_3Ge compositions and manganese carbide. In the C 1s spectrum, apart from the line of carbon contaminations (285.0 eV), there is a band of graphitized carbon (284.5 eV) and a line typical of carbides (283.2 eV) (Fig. 4e). Carbon is present in the samples even after prolonged ion etching to a depth of ~50 nm. The obtained XPS and magnetic data confirm that carbon and oxygen inclusions contained in the 20Ge/80Mn sample are incorporated into the Mn_5Ge_3 lattice after annealing at 500 °C; this significantly affects the magnetic properties.

The XPS data are consistent with X-ray and magnetic results that show the formation of Mn_5Ge_3 and MnO after annealing at 500 °C. It is known that Mn_5Ge_3 belongs to the Nowotny phases [40], in which impurity atoms such as C, N, and O are incorporated into Mn_5Ge_3 interstitial sites with no significant change in the lattice parameter. Indirect evidence of the incorporation of C atoms and the formation of the C-doped Mn_5Ge_3 films is seen in the lattice compression compared to the Mn_5Ge_3 lattice. The lattice parameters determined from the diffraction lines are $c = 5.013$ nm and $a = 7.164$ nm. The ratio $c/a = 0.700$ coincides with the value for the $Mn_5Ge_3C_{0.75}$ films [17]. The C-doping effect has been intensively studied, whereas there is a lack of data in the literature on the effect of oxygen impurities on the magnetic properties of the Mn_5Ge_3 films. Calculations show that magnetic properties strongly degrade and can be even suppressed as the oxygen content increases [33]. An experimental study of the $Ge_{0.99}Mn_{0.01}$ nanowires containing Mn–O structures yields the Curie temperature $T_C > 300$ K, which is higher than that of the Mn_5Ge_3 phase. However, the nature of this ferromagnetic behavior is not clearly understood [41]. The above arguments support the idea that not only C but also O impurity atoms, incorporated into the octahedral interstitial sites of the Mn_5Ge_3 lattice with the formation of the $Mn_5Ge_3C_xO_y$ phase, can change the Curie temperature and saturation magnetization. Therefore, we believe that the formation of the ferromagnetic $Mn_5Ge_3C_xO_y$ clusters is the real nature of the observed magnetization and Curie temperature growth in the 20Ge/80Mn films after annealing at 500 °C. Based on the above structural and magnetic results, we propose the following physical

picture of phase formation in 20Ge/80Mn samples upon annealing at temperatures up to 500 °C. At ~120 °C, the ferromagnetic Mn_5Ge_3 phase first forms at the Ge/Mn interface, and the fraction of this phase grows as the temperature increases to ~250 °C. Upon annealing at ~250 °C, only the Mn_5Ge_3 phase and the unreacted Mn layer remain in the sample. Above 250 °C, the solid-state reaction between Mn_5Ge_3 and Mn begins and leads to the sequential formation of the weak magnetic Mn_5Ge_2 (71.43%Mn) and Mn_3Ge (75%Mn) phases:

$$Mn_5Ge_3 + Mn \rightarrow Mn_5Ge_2, Mn_5Ge_2 + Mn \rightarrow Mn_3Ge. \quad (1)$$

This makes the sample weakly magnetic after annealing at 350 °C. Upon annealing at temperatures above 400 °C, the gas impurities – mainly C and O, which have so far been chemically inert – start interacting with Mn. Oxygen penetrating into the Mn_5Ge_2 and Mn_3Ge lattices partially oxidizes Mn to MnO. This causes the reaction back to reaction (1) and there is secondary formation of the ferromagnetic Mn_5Ge_3 phase. Similar to the C-doping of the Mn_5Ge_3 films, the formation of the $Mn_5Ge_3C_xO_y$ clusters occurs via carbon and oxygen migration to the Mn_5Ge_3 lattice, which increases magnetization and the Curie temperature of the sample. Note that the films were annealed in a vacuum at a residual pressure of 10^{-4} Pa. At this condition residual oxygen contamination can actively participate in the formation of oxides. However, the effect of oxygen contamination on the synthesis of the Mn_5Ge_3 phase cannot be prevented even in an ultra-high vacuum [32,42,43].

It is known that solid-state reactions in thin films occur at low temperatures. As the annealing temperature increases, only one (first) phase forms at the interface. Further increases in temperature lead to the formation of a phase sequence. To date, the formation of the first phase and phase sequence and the temperatures of their initiations have not been grounded, although several models have been proposed [see 44–47 and references therein]. Recently, we demonstrated the formation of the 80Ge/20Mn → (~120 °C) Mn_5Ge_3 → (~300 °C) $Mn_{11}Ge_8$ phase sequence upon heating to 400 °C [18]. It can be seen that the Mn_5Ge_3 phase forms first at the Ge/Mn interface, independent of the Ge and Mn film thicknesses. This conclusion is consistent with the results reported in Wittmer et al. [48]. The initiation temperature of the solid-state synthesis of the Mn_5Ge_3 phase (~120 °C) is close to the temperature of the spinodal decomposition of the $Mn_{1-x}Ge_x$ ($x > 0.95$) solid solution. These results in the formation of Mn_5Ge_3 precipitates embedded in the Ge-rich matrix [21–26]. Our previous work clearly suggests that many thin film solid-state reactions start at temperatures of solid phase transformations. In particular, solid-state reactions in Ni/Fe and Fe/Cu films start at temperatures of ~620 K and ~850 °C, which correspond to the temperatures of eutectoid decompositions in Ni–Fe [49] and Cu–Fe [50] systems, respectively. The experimental coincidence of these temperatures suggests the presence of common chemical mechanisms for the solid-state synthesis of Mn_5Ge_3 and phase separation in the $Mn_{1-x}Ge_x$ films. Above 120 °C, strong chemical interactions between Mn and Ge lead to the formation of the first Mn_5Ge_3 phase, independent of whether Mn and Ge atoms are in a solid solution or in Ge/Mn bilayers. It should be emphasized that during the formation of the Mn_5Ge_3 phase in the spinodal decomposition, the atoms migrate a distance of several nanometers, while in the solid-state synthesis they migrate to a depth comparable with the thickness of a Mn or Ge layer (i.e., over 200 nm). These results provide an unprecedented view of the solid-state reaction between Mn and Ge and its position in the nature of the spinodal decomposition of the $Mn_{1-x}Ge_x$ solid solution.

We believe that the Mn_5Ge_3 phase is thermodynamically stable at low temperatures. Above 300 °C, the Mn_5Ge_3 phase transforms to $Mn_{11}Ge_8$ in a solid-state reaction with the Ge layer [18], or to Mn_5Ge_2 and Mn_3Ge in reactions with Mn, according to Reaction (1). These results contradict the data reported in previous studies [6–8,51], in which the authors suggest that the Mn_5Ge_3 phase is unstable and can be stabilized during epitaxial growth on Ge (111) substrates. The Mn_5Ge_3 phase also forms first during the sequential deposition of Mn and Ge onto the Ge and Mn layers, respectively, at temperatures above 120 °C. The doping temperature of Ge under Mn implantation can exceed the initiation temperature of 120 °C. Therefore, one can expect the formation of Mn_5Ge_3, $Mn_{11}Ge_8$, Mn_5Ge_2, and Mn_3Ge nanoclusters upon Mn implantation in Ge wafers and subsequent annealing. Yoon [52] reported the formation of the Mn_5Ge_3 phase through the implantation of Mn into Ge quantum dots with subsequent annealing at 650 °C. The polycrystalline Mn_5Ge_2 phase is formed by implantation of Mn into (001) Ge wafers and pulsed laser annealing with a pulse duration of 300 ns [53].

3. Conclusions

We performed a systematic study of the solid-state reactions between Mn and Ge films with the nominal atomic ratio 80Mn:20Ge at temperatures from 50 to 500 °C. It is established that above 120 °C, the ferromagnetic Mn_5Ge_3 phase grows at the Ge/Mn interface to 250 °C. Only the Mn_5Ge_3 phase and the residual Mn layer are present in the reaction products. Upon annealing at temperatures above 250 °C, the Mn_5Ge_3 phase starts to react with Mn with the sequential formation of the Mn_5Ge_2 and Mn_3Ge phases. These make the sample weakly magnetic. The repeated occurrence of magnetization and the Mn_5Ge_3 reflections are observed upon annealing at 400 °C. The photoelectron spectra and magnetic measurements indicate the migration of C and O into the Mn_3Ge lattice and the formation of the Nowotny phase $Mn_5Ge_3C_xO_y$ with the Curie temperature T_C ~ 350–360 K and the high saturation magnetization M_S ~ 14–25 kA/m at room temperature.

References

[1] S. Picozzi, A. Continenza, A.J. Freeman, Phys. Rev. B 70 (2004) 235205.
[2] C. Zeng, S.C. Erwin, L.C. Feldman, A.P. Li, R. Jin, Y. Song, J.R. Thompson, H.H. Weitering, Appl. Phys. Lett. 83 (2003) 5002.
[3] S. Olive-Mendez, A. Spiesser, L.A. Michez, V. Le Thanh, A. Glachant, J. Derrien, T. Devillers, A. Barski, M. Jamet, Thin Solid Films 517 (2008) 191.
[4] R.P. Panguluri, C. Zeng, H.H. Weitering, J.M. Sullivan, S.C. Erwin, B. Nadgorny, Phys. Status Solidi B 242 (2005) R67.
[5] M.-T. Dau, V.L. Thanh, T.-G. Le, A. Spiesser, M. Petit, L.A. Michez, R. Daineche, Appl. Phys. Lett. 99 (2011) 151908.
[6] A. Spiesser, V.L. Thanh, S. Bertaina, L.A. Michez, Appl. Phys. Lett. 99 (2011) 121904.
[7] A. Spiesser, I. Slipukhina, M.-T. Dau, E. Arras, V. Le Thanh, L. Michez, P. Pochet, H. Saito, S. Yuasa, M. Jamet, J. Derrien, Phys. Rev. B 84 (2011) 165203.
[8] A. Spiesser, S.F. Olive-Mendez, M.-T. Dau, L.A. Michez, A. Watanabe, V. Le Thanh, A. Glachant, J. Derrien, A. Barski, M. Jamet, Thin Solid Films 518 (2010) S113.
[9] M.-T. Dau, A. Spiesser, T. Le Giang, L.A. Michez, S.F. Olive-Mendez, V. Le Thanh, M. Petit, J.-M. Raimundo, A. Glachant, J. Derrien, Thin Solid Films 518 (2010) S266.
[10] J.H. Grytzelius, H.M. Zhang, L.S.O. Johansson, Phys. Rev. B 84 (2011) 195306.
[11] P. De Padova, J.-M. Mariot, L. Favre, I. Berbezier, B. Olivieri, P. Perfetti, C. Quaresima, C. Ottaviani, A. Taleb-Ibrahimi, P. Le Fèvre, F. Bertran, O. Heckmann, M.C. Richter, W. Ndiaye, F. D'Orazio, F. Lucari, C.M. Cacho, K. Hricovini, Surf. Sci. 605 (2011) 638.
[12] C. Sürgers, K. Potzger, T. Strache, W. Möller, G. Fischer, N. Joshi, H.v. Löhneysen, Appl. Phys. Lett. 93 (2008) 062503.
[13] I. Slipukhina, E. Arras, Ph. Mavropoulos, P. Pochet, Appl. Phys. Lett. 94 (2009) 192505.
[14] C. Sürgers, K. Potzger, G. Fischer, J. Chem. Sci. 121 (2009) 173.
[15] N. Stojilovic, S.V. Dordevic, Rongwei Hu, C. Petrovic, J. Appl. Phys. 114 (2013) 053708.
[16] M. Petit, M.T. Dau, G. Monier, L. Michez, X. Barre, A. Spiesser, V.L. Thanh, A. Glachant, C. Coudreau, L. Bideux, C. Robert-Goumet, Phys. Status Solidi C 9 (2012) 1374.
[17] M. Gajdzik, C. Sürgers, J. Magn. Magn. Mater. 221 (2000) 248.
[18] V.G. Myagkov, V.S. Zhigalov, A.A. Matsynin, L.E. Bykova, G.V. Bondarenko, G.N. Bondarenko, G.S. Patrin, D.A. Velikanov, JETP Lett. 96 (2012) 40.
[19] O. Abbes, F. Xu, A. Portavoce, C. Girardeaux, K. Hoummada, V. Le Thanh, Solid State Phenom. 172–174 (2011) 579.
[20] C. Zeng, W. Zhu, S.C. Erwin, Z. Zhang, H.H. Weitering, Phys. Rev. B 70 (2004) 205340.
[21] J.-P. Ayoub, L. Favre, I. Berbezier, A. Ronda, L. Morresi, N. Pinto, Appl. Phys. Lett. 91 (2007) 141920.

[22] R.T. Lechner, V. Holý, S. Ahlers, D. Bougeard, J. Stangl, A. Trampert, A. Navarro-Quezada, G. Bauer, Appl. Phys. Lett. 95 (2009) 023102.
[23] F. Xiu, Y. Wang, K. Wong, Y. Zhou, X. Kou, J. Zou, Nanotechnology 21 (2010) 255602.
[24] A. Jain, M. Jamet, A. Barski, T. Devillers, I.-S. Yu, C. Porret, P. Bayle-Guillemaud, V. Favre-Nicolin, S. Gambarelli, V. Maurel, G. Desfonds, J.F. Jacquot, S. Tardif, J. Appl. Phys. 109 (2011) 013911.
[25] E. Biegger, L. Stäheli, M. Fonin, U. Rüdiger, Yu.S. Dedkov, J. Appl. Phys. 101 (2007) 103912.
[26] S. Yada, P.N. Hai, S. Sugahara, M. Tanaka, J. Appl. Phys. 110 (2011) 073903.
[27] N. Yamada, H. Sakai, H. Mori, T. Ohoyama, Physica B 149 (1988) 311.
[28] H. Kurt, N. Baadji, K. Rode, M. Venkatesan, P. Stamenov, S. Sanvito, J.M.D. Coey, Appl. Phys. Lett. 101 (2012) 132410.
[29] D.D. Dung, W. Feng, Y. Shin, S. Cho, J. Appl. Phys. 109 (2011) 07C310.
[30] T. Matsui, M. Shigematsu, S. Mino, H. Tsuda, H. Mabuchi, K. Morii, J. Magn. Magn. Mater. 192 (1999) 247.
[31] T. Ohoyama, J. Phys. Soc. Jpn. 16 (1961) 1995.
[32] W. Yin, C.D. Kell, L. He, M.C. Dolph, C. Duska, J. Lu, R. Hull, J.A. Floro, S.A. Wolf, J. Appl. Phys. 111 (2012) 033916.
[33] A. Continenza, G. Profeta, Phys. Rev. B 78 (2008) 085215.
[34] Y.-F. Qin, S.-S. Yan, S.-Q. Xiao, Q. Li, Z.-K. Dai, T.-T. Shen, S.-S. Kang, Y.-Y. Dai, G.-L. Liu, Y.-X. Chen, L.-M. Mei, J. Appl. Phys. 109 (2011) 083906.
[35] H.W. Nesbitt, D. Banerjee, Am. Mineral. 83 (1998) 305.
[36] M.C. Biesinger, B.P. Payne, A.P. Grosvenor, L.W.M. Lau, A.R. Gerson, R.St.C. Smart, Appl. Surf. Sci. 257 (2011) 2717.
[37] S.-P. Jeng, R.J. Lad, V.E. Henrich, Phys. Rev. B 43 (1991) 11971.
[38] B. Schmid, A. Müller, M. Sing, R. Claessen, J. Wenisch, C. Gould, K. Brunner, L. Molenkamp, W. Drube, Phys. Rev. B 78 (2008) 075319.
[39] P. De Padova, J.-P. Ayoub, I. Berbezier, P. Perfetti, C. Quaresima, A.M. Testa, D. Fiorani, B. Olivieri, J.-M. Mariot, A. Taleb-Ibrahimi, M.C. Richter, O. Heckmann, K. Hricovini, Phys. Rev. B 77 (2008) 045203.
[40] J.D. Corbett, E. Garcia, A.M. Guloy, W.-M. Hurng, Y.-U. Kwon, E.A. Leon-Escamilla, Chem. Mater. 10 (1998) 2824.
[41] J.S. Kulkarni, O. Kazakova, D. Erts, M.A. Morris, M.T. Shaw, J.D. Holmes, Chem. Mater. 17 (2005) 3615.
[42] P. De Padova, J.-P. Ayoub, I. Berbezier, J.-M. Mariot, A. Taleb-Ibrahimi, M.C. Richter, O. Heckmann, A.M. Testa, D. Fiorani, B. Olivieri, S. Picozzi, K. Hricovini, Surf. Sci. 601 (2007) 2628.
[43] P. Gambardella, L. Claude, S. Rusponi, K.J. Franke, H. Brune, J. Raabe, F. Nolting, P. Bencok, A.T. Hanbicki, B.T. Jonker, C. Grazioli, M. Veronese, C. Carbone, Phys. Rev. B 75 (2007) 125211.
[44] In: J.M. Poate, K.N. Tu, J.W. Mayer (Eds.), Willey-Interscience, New York, 1978.
[45] E.G. Colgan, Mater. Sci. Rep. 5 (1990) 1.
[46] R. Pretorius, C.C. Theron, A. Vantomme, J.W. Mayer, Crit. Rev. Solid State Mater. Sci. 24 (1999) 1.
[47] T. Laurila, J. Molarius, Crit. Rev. Solid State Mater. Sci. 28 (2003) 185.
[48] M. Wittmer, M.-A. Nicolet, J.W. Mayer, Thin Solid Films 42 (1977) 51.
[49] V.G. Myagkov, V.C. Zhigalov, L.E. Bykova, G.N. Bondarenko, J. Magn. Magn. Mater. 305 (2006) 534.
[50] V.G. Myagkov, O.A. Baykov, L.E. Bykova, G.N. Bondarenko, J. Magn. Magn. Mater. 321 (2009) 2260.
[51] M.-T. Dau, V. Le Thanh, L.A. Michez, M. Petit, T.-G. Le, O. Abbes, A. Spiesser, A. Ranguis, New J. Phys. 14 (2012) 103020.
[52] I.T. Yoon, J. Supercond. Nov. Magn. 23 (2010) 319.
[53] D. Bürger, S. Zhou, M. Höwler, X. Ou, G.J. Kovacs, H. Reuther, A. Mücklich, W. Skorupa, M. Helm, H. Schmidt, Appl. Phys. Lett. 100 (2012) 012406.